Proceedings of the Fourth Lunar Science Conference
(Supplement 4, *Geochimica et Cosmochimica Acta*)
Vol. 1, pp. 481–504

Apollo 16 rocks: Classification and petrogenetic model

JEFFREY L. WARNER
NASA Johnson Space Center, Houston, Texas 77058

CHARLES H. SIMONDS
Lunar Science Institute, Houston, Texas 77058

WILLIAM C. PHINNEY
NASA Johnson Space Center, Houston, Texas 77058

Abstract—The Apollo 16 rocks include cataclastic anorthosites, two varieties of unequilibrated breccia, two varieties of partly- to fully-equilibrated breccia, and a sequence of partially melted breccias. The latter, which dominate the Apollo 16 collection, include glass, devitrified glass, mesostasis-olivine-plagioclase rock, mesostasis-rich basalt, basalt, and poikilitic rocks. All sequence members contain vesicles and relics of plagioclase, olivine, pink spinel, and lithic fragments. Their equilibrated matrices define a series from glass, to a plagioclase–olivine–mesostasis assemblage displaying spherulitic and skeletal shaped crystals, through a plagioclase–pyroxene–olivine assemblage displaying euhedral shaped crystals. Such data suggest that the sequence lithologies were derived from breccias or soils that were partially melted in an impact event. The product of the melting was a liquid that contained the solid material that we now observe as the relics. The range in mineralogy and texture in the sequence lithologies is due to different cooling rates—the glass end of the sequence cooled rapidly whereas the crystalline end cooled more slowly.

INTRODUCTION

APOLLO MISSIONS 14, 16, and 17 have shown that the lunar highlands consist of petrologically complex rocks (LSPET, 1971, 1973a, 1973b). Textural evidence suggests that at one time most of the highland rocks were polymict glassy breccias or soils, similar to those found at the Apollo 11, 12, and 15 sites. However, most highland "breccias" are now holocrystalline and show few mineralogic and micro-textural similarities to their supposed protoliths. The prime object of this study is to decipher and petrologic processes that are responsible for the present mineralogy and texture of these crystalline breccias.

Our method is to petrographically study a large number of samples. From these data a genetic classification is constructed by assigning the chief lithology(s) in each sample to a group. Most important is that this classification scheme recognizes a genetic sequence among the groups. The petrogenesis of each group, and sequence of groups, is then interpreted in the context of the total system, taking into account the detailed mineralogic and textural characteristics of the various groups. This method has been successfully applied to the Apollo 14 metamorphosed breccias by Warner (1972). It is generally known as a "lumped parameter process-response model" (Domenico, 1972), where the rocks are the "response"

and the petrogenesis is the "process." Lumped parameter means that all inputs to the model are combined into one factor. In this case we lump the petrographic descriptions into the one parameter considered. Thus, no account is taken of the details of the samples formation or exposure ages, nor its stratigraphic or geographic position.

The samples available for detailed petrographic and microprobe studies of mineral chemistry and limited bulk chemistry were rake samples. Fifty-three fragments were thin sectioned from the Apollo 16 rake samples from Stations 1 (615XX's), 4 (645XX's and 648XX's), and 13 (635XX's). In addition, thin sections of 63 other Apollo 16 rocks were studied petrographically in the Curator's laboratories. Hand specimen descriptions for all the rake samples from Stations 1, 4, and 13 are available from the Lunar Sample Curator's Office at the NASA Johnson Space Center. Accompanying studies on the same samples consider the petrology and origin of the poikilitic rocks (Simonds *et al.*, 1973) and the phase relations of Fe–Ni metal and schreibersite (Gooley *et al.*, 1973).

CLASSIFICATION

The 116 Apollo 16 samples that were studied in thin section fit into the groups and subgroups as set out in Table 1. Table 2 contains the lithic assignments for each rock. The Curator's photographs of the fresh exterior surface of each rock were studied in order to determine the megascopic relations of the microscopically determined lithologies. Those rocks where the clast-host relations are not clear are classed as black and white rocks in Table 2. The black and white rocks are equivalent to some of PET's partially molten breccias (LSPET, 1973a) and to

Table 1. Classification scheme for Apollo 16 rocks.

Cataclastic Anorthosite		
Breccias		
Light Matrix Breccia (LMB)		
Glassy Breccia		
Metamorphosed Breccia		
Meta-norite		
Melted Matrix Breccia		
Glass		Glassy end of the Petrogenetic Sequences
Mesostasis-Rich Rocks		
Devitrified Glass		
Spherulitic Devitrified Glass		
Dendritic Devitrified Glass		
Mesostasis–Olivine–Plagiocase (M–Ol–P) Rock	The Petrogenetic Sequence	
Mesostasis-Rich Basalt Petrogenetic		
Basalts		
Porphyritic Basalts		
Quench Basalts		
Metamorphosed Basalts		Crystalline end of the Petrogenetic Sequence
Mafic Basalts		
Poikilitic Rocks		

Table 2. Classification of Apollo 16 rocks.

60015	Cataclastic anorthosite with devitrified glass coating
60016	Light matrix breccia or cataclastic anorthosite with clasts
60017	Devitrified glass to melted matrix shocked breccia
60018	B&W*; cataclastic anorthosite plus mesostasis-rich basalt and basalt
60019	Glassy breccia
60025	Cataclastic anorthosite
60115	B&W breccia: light matrix breccia plus?
60215	Cataclastic anorthosite
60255	Glassy breccia with lots of poikilitic clasts
60275	Glassy breccia
60315	Poikilitic
60335	Basalt
61015	B&W: cataclastic anorthosite plus mesostasis-rich basalt
61016	B&W: cataclastic anorthosite plus mesostasis-rich basalt
61135	Light matrix breccia
61155	Light clast is light matrix breccia
61156	B&W:? cataclastic anorthosite plus poikilitic
61295	Glassy breccia to melted matrix breccia
61516	Light matrix breccia
61525	Glassy breccia
61535	Glassy breccia, very glass rich
61538	Dendritic devitrified glass
61546	Dendritic devitrified glass to melted matrix breccia
61547	Spherulitic devitrified glass with basalt clasts
61548	Melted matrix breccia
61549	Meta-basalt with meta-norite clast
61556	Dendritic devitrified glass
61558	Spherulitic devitrified glass
61559	Partly devitrified glass to very glassy breccia
61568	Poikilitic with clasts of feldspathic basalt
61569	Poikilitic
61575	Devitrified glass(?) with large clear plagioclase clasts
61577	Meta-norite with glass rim
62235	Poikilitic
62236	Cataclastic anorthosite
62237	Cataclastic anorthosite
62275	Light matrix breccia
62295	Mesostasis-rich basalt
63335	Devitrified glass plus mesostasis-rich basalt (?)
63505	Meta-norite
63506	Meta-basalt
63507	Glassy breccia
63535	Basalt
63538	Dendritic devitrified glass plus melted matrix breccia
63545	Basalt
63547	Poikilitic
63549	Porphyritic basalt
63556	Poikilitic
63557	Meta-norite
63558	Poikilitic

*B&W—black and white rock.

Table 2. (continued).

63566	Dendritic to spherulitic devitrified glass
63575	Glass-cementing light clasts
63578	Slightly metamorphosed glassy breccia
63585	Basalt
63589	Glassy breccia
63598	Micro-norite type mafic basalt
64435	B&W: cataclastic anorthosite plus meta-basalt
64455	Glass coated basalt
64477	B&W: cataclastic anorthosite to light matrix breccia plus mesostasis-rich basalt
64535	B&W: cataclastic anorthosite plus mesostasis–olivine–plagioclase rock
64537	B&W: cataclastic anorthosite plus mesostasis–olivine–plagioclase rock
64546	B&W: cataclastic anorthosite plus mesostasis–olivine–plagioclase rock to basalt
64548	Light matrix breccia
64559	B&W: cataclastic anorthosite plus mesostasis-rich basalt
64565	Spherulitic to dendritic devitrified glass
64567	Poikilitic to basalt
64568	Poikilitic
64569	Poikilitic
64575	Poikilitic
64576	Meta-breccia with veins of mafic basalt
64577	Dendritic to spherulitic devitrified glass
64579	Dendritic to spherulitic devitrified glass
64585	Mesostasis-rich basalt
64586	Mesostasis–olivine–plagioclase rock
64587	Glassy breccia
64588	Glassy breccia
64815	Meta-poikilitic
64816	Poikilitic
64817	Basalt
64818	Meta-norite
64819	Cataclastic anorthosite with glass veins
64826	Glassy breccia
64827	Glassy breccia
65015	Poikilitic
65035	B&W: cataclastic anorthosite plus fine-grained mesostasis-rich basalt
65055	Porphyritic basalt
65056	Devitrified glass with clasts of cataclastic anorthosite
65075	Cataclastic anorthosite plus basalt—glass coated
65095	Light matrix breccia with many lithic clasts
65315	Cataclastic anorthosite with glass veins
66035	Glassy breccia to light matrix breccia
66036	Light matrix breccia
66055	Light matrix breccia
66095	Basalt
67015	Light matrix breccia with many lithic clasts
67016	Glassy breccia to light matrix breccia
67025	Basalt
67035	Light matrix breccia
67075	Cataclastic anorthosite
67415	Cataclastic anorthosite
67435	Poikilitic with partly devitrified glass coating
67455	Glassy breccia to light matrix breccia

Table 2. (continued).

67735	Cataclastic anorthosite with clasts
67915	Light matrix breccia to glassy breccia
67936	Meta-breccia clasts cemented by glass
67937	Mesostasis-rich basalt
67945	Poikilitic to basalt—one of several fragments
67946	Devitrified glass
67948	Mesostasis-rich basalt
67955	Light matrix breccia
67956	Mesostasis-rich basalt
67975	Most clasts are light matrix breccia
68115	Devitrified glass
68415	Porphyritic basalt
68416	Porphyritic basalt
68815	Devitrified glass

some of the B2, B3, and B4 breccias of Wilshire *et al.* (1973). The various lithologies making up each black and white rock are listed in Table 2, where the individual lithologies are separated with a "plus." For example, 61015 is a black and white rock consisting of cataclastic anorthosite and mesostasis-rich basalt.

Cataclastic anorthosite

Cataclastic anorthosites are white rocks that contain over 90% plagioclase with minor amounts of olivine, orthopyroxene, and/or diopsidic augite. Similar rocks have been described by Phinney *et al.* (1972), James (1972), and others from Apollo 15. The plagioclase in cataclastic anorthosites occur in two forms: as large irregular crystals (up to several centimeters across) that display internal fracturing, and as small irregular angular crystals that are the matrix for the large crystals (Fig. 1a). Cataclastic anorthosites grade into the light matrix breccias described below.

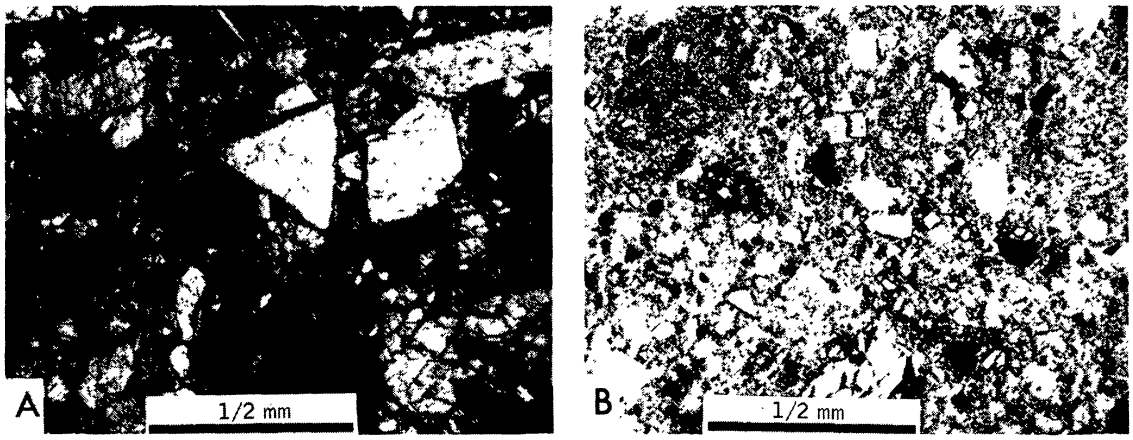

Fig. 1. Photomicrographs of anorthositic rocks. (a) Cataclastic anorthosite part of black and white rock 64535 in partly polarized light; (b) Light matrix breccia 61516. Note the fragmental nature of this rock in contrast to the cataclastic anorthosite.

Breccias

The term breccia is used in this paper in two ways. First, there is a lithology. A breccia must be polymict, i.e., it must contain various types of lithic clasts besides containing mineral clasts. Also, a breccia contains an unequilibrated matrix, i.e., the matrix contains glass, angular particles, displays a wide range of compositions for each mineral species, and contains large amounts of pore space (up to 30%) distributed as micron-size cavities. Such rocks were described as low-grade breccias by Warner (1972) from the Apollo 14 collection and as welded breccias by McKay and Morrison (1971) from the Apollo 11 and 12 collections. The second use of breccia is in a generic sense when referring to all the Apollo 16 rocks as a group, or when referring to the protolith of a melted or metamorphosed rock that, at one stage in its history, was a breccia in the former sense.

Light matrix breccia. Light matrix breccias are white to light tan breccias that were first described by Delano *et al.* (1973). Light matrix breccias contain lithic clasts and rounded to subrounded plagioclase, pyroxene, and olivine clasts in a texturally and mineralogically unequilibrated matrix (Fig. 1b). These rocks all contain light orange-brown glass in the matrix and as wispy and rounded clasts. The Apollo 14 white rocks (14063, 14064, and 14082) described by Warner (1972) are light matrix breccias. Note that Delano's use of light matrix breccia includes both unrecrystallized and recrystallized members whereas in this paper only unrecrystallized members are included. Light matrix breccias grade into glassy breccias described below.

Glassy breccia. Glassy breccias are dark brown to dark gray breccias. These rocks are called dark matrix breccias by Delano *et al.* (1973) and are similar to the Apollo 11 and 12 breccias as described by McKay and Morrison (1971) and to the low-grade Apollo 14 breccias as described by Warner (1972). These rocks contain lithic fragments, glass, plagioclase, pyroxene, olivine, and metal as rounded to angular clasts. The matrix of the glassy breccias consist of large amounts (about 50%) of brown glass. The remainder of the matrix consists of angular fragments of glass, ilmenite, and the clast minerals. Glassy breccias have a texturally and mineralogically unequilibrated matrix.

Metamorphosed breccia. Metamorphosed breccias are polymict rocks—they contain rounded to subrounded lithic and mineral clasts. They contain no glass and have a fine-grained, ragged, granoblastic matrix. These rocks, and most of the lithologies described below, contain partly- to fully-equilibrated matrices. Glass does not occur in these rocks, nor does it occur in other lithologies with a partly- to fully-equilibrated matrix. The Apollo 16 metamorphosed breccias display a range of matrix textures: most are texturally similar to the medium-grade Apollo 14 metamorphic breccias and some texturally resemble the high-grade Apollo 14 metamorphic breccias (medium- and high-grade Apollo 14 breccias described by Warner, 1972). In all cases, each matrix mineral species (pyroxene, olivine, and plagioclase) tends to be of equal size throughout a thin section. This suggests tex-

tural equilibrium is being approached. The shape of the matrix plagioclase tends to be equant, suggesting solid state recrystallization.

A special variety of metamorphosed breccia that lack lithic clasts and has a well developed annealed texture is known as meta-norite. Meta-norites do contain mineral clasts. Plagioclase forms a tightly packed network of equant crystals that meet at 120° corners. The mafic minerals (low-Ca pyroxene with minor amounts of augite and/or olivine) form small (about $\frac{1}{3}$ to $\frac{1}{10}$ the size of the plagioclase), rounded crystals that are located along the grain boundaries of the plagioclase network. The meta-norites have a distinctive "salt and pepper" appearance. Meta-norites were first described from the Apollo 15 collection by Cameron *et al.* (1973). Many of the anorthosite and anorthositic gabbro fragments described from Apollo 11 by Wood *et al.* (1970) would be classed as meta-norites (e.g., Wood's Figs. 3a, 3b, and 4a).

Melted matrix breccia. Melted matrix breccias are glassy breccias and metamorphosed breccias that contain regions within their matrix consisting of a mosaic of tablet-shaped plagioclase crystals and interstitial brown mesostasis (Fig. 2). The mesostasis is cryptocrystalline, consisting of pyroxene, ilmenite, metal, and a Si-rich phase (glass). The plagioclase tablets and the interstitial patches of mesostasis range in grain size within each region of this "melted" texture; the plagioclase tablets ranging in length from 4 to 100 microns. Where this texture is coarsest, it is similar to the dendritic devitrified glass described below. At the edges of these regions, the "melted" texture grades imperceptibly into the breccias' normal matrix. In sample 61548, the entire matrix displays this "melted" texture.

Melted matrix breccias are important in this genetic classification as they are texturally transitional between normal breccias and various petrogenetic sequence breccias (glass, devitrified glass, mesostasis–olivine–plagioclase rocks, mesostasis-rich basalts, basalts, and poikilitic rocks) described below. We suggest that the melted matrix breccias are a half-way product of the same impact melting

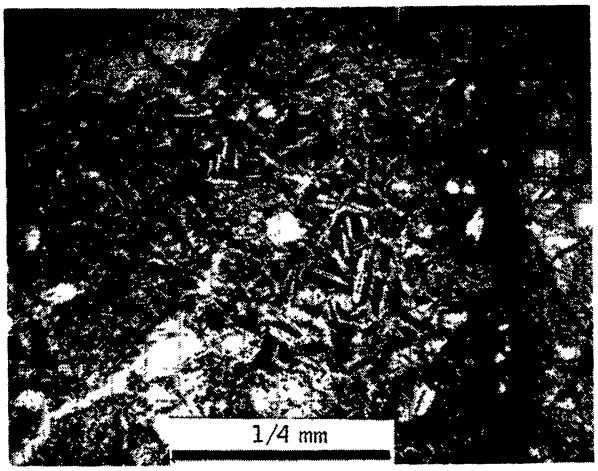

Fig. 2. Photomicrograph of melted matrix breccia 61548. Note the change in grain size of the matrix across the photo.

processes that produced the petrogenetic sequence breccias. Melted matrix breccias grade into devitrified glass.

Glass

Several centimeter-sized samples that consist of glass are present among the Apollo 16 samples. The glass contains spherical vesicles and rare plagioclase relics, the latter are less than 200 microns across. In most glass samples, the glass can be traced imperceptibly into glassy breccia. The glass is dark brown to reddish brown in color and has an internal structure defined by light and dark bands. The color in the dark bands is due to numerous < 1 micron blebs of metal. Flow banding is observed. Workers who study soil petrography would call these samples agglutinates.

Mesostasis-rich rocks

Devitrified mesostasis–olivine–plagioclase rock (M–Ol–P), and mesostasis-rich basalt are the names given to three holocrystalline lithologies found at Apollo 16 that all have the same essential matrix mineralogy: plagioclase, olivine, and mesostasis. Mesostasis is a very fine-grained (< 1 micron) intergrowth of crystals and/or glass. All lithologies contain mineral clasts, lithic clasts, and vesicles. The three lithologies define a continuum in texture, relic population, and matrix mode. The mineralogy of these rocks is set out in Table 3.

Devitrified glass. The matrix texture of devitrified glass is not basaltic. Rather it is characterized by regions of olivine and/or mesostasis that are separated by plagioclase crystals (Figs. 3a, b). In dendritic devitrified glass, plagioclase occurs as tablets up to 300 microns long. Within polygonal areas (100×600 microns) and plagioclase tablets form parallel sets (Fig. 3a). In contrast the plagioclase in spherulitic devitrified glass does not occur in parallel sets, rather the plagioclase forms accicular crystals that range from 50 to 150 microns in length (Fig. 3b). Small sets of crystals form fan and bow-tie patterns, commonly nucleated on the edges of relic feldspar grains.

Table 3. Mineralogy of the mesostasis-rich rocks.

		Devitrified Glass	M–Ol–P Rocks	Mesostasis-Rich Basalts
Matrix	Plagioclase	An_{94-97}	An_{92-95}	An_{88-96}
	Olivine	Fo_{75-79}	Fo_{75-78}	Fo_{74-81} (zoned)
	Mesostasis contains	High-Ca pigeonite	?	High-Ca pigeonite
		Fe–Ti oxide	Fe–Ti oxide	Fe–Ti oxide
		Metal	Metal	Metal
	Other phases			Mg–Al spinel
Relics Assemblage		Lithic Plagioclase	Lithic Plagioclase Spinel	Lithic Plagioclase Spinel Olivine

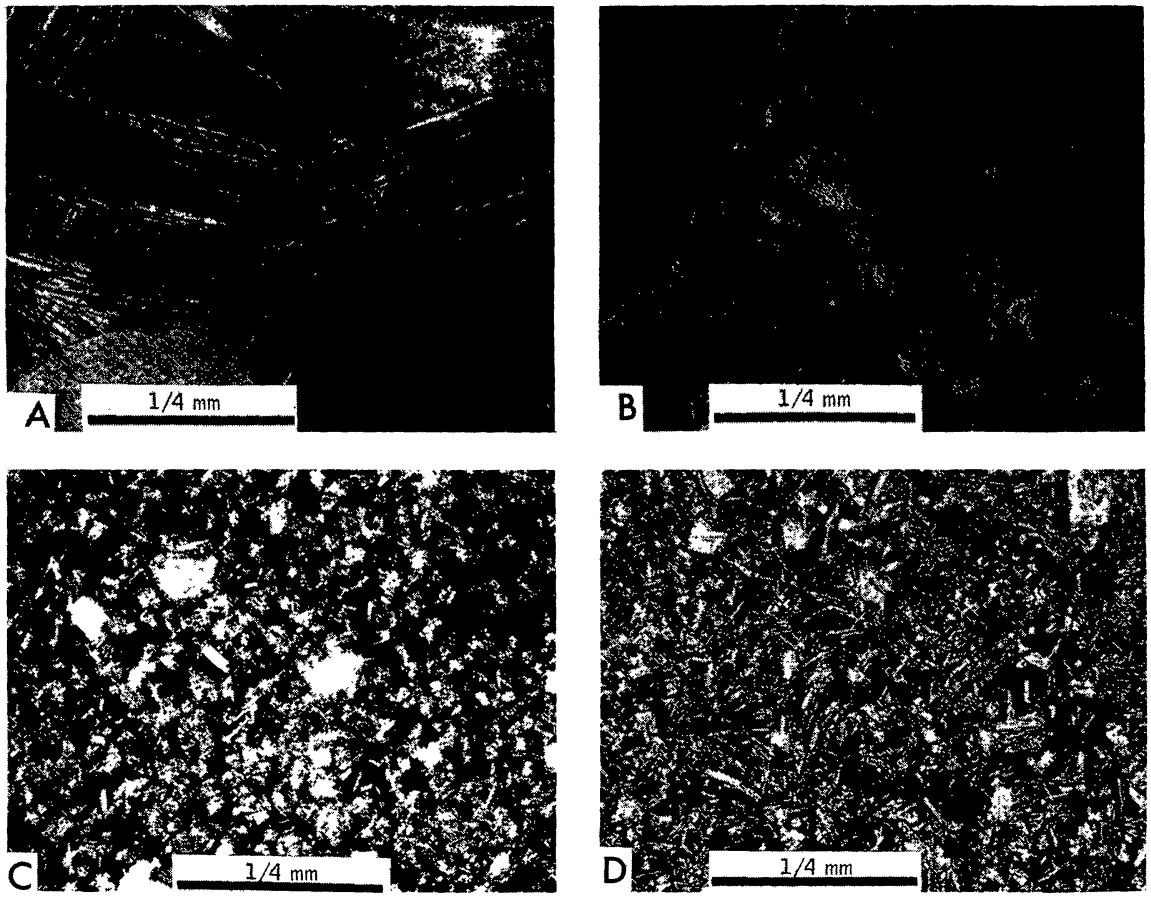

Fig. 3. Photomicrographs of mesostasis-rich rocks. (a) Dendritic devitrified glass 61556; (b) Spherulitic devitrified glass 61558; (c) M–Ol–P rock part of black and white rock 64535; and (d) Mesostasis-rich basalt 64559. These rocks do not contain pyroxene crystals.

Plagioclase in the devitrified glasses range from An_{94} to An_{97}. It forms as skeletal dendritic to spherulitic crystals, i.e., crystals typical of quench products with large amounts of under-cooling below the liquidus (Lofgren, 1973). Anhedral olivine (Fo_{75-79}) crystals occur between plagioclase crystals. The mesostasis is cryptocrystalline, consisting of high-Ca pigeonite (about $Wo_{15}En_{65}Fs_{20}$), ilmenite or armalcolite, Cr-spinel(?), metal, and glass.

Relics are not common in the devitrified glasses but a few subrounded plagioclase grains and rare lithic fragments are found.

Devitrified glasses grade into M–Ol–P rocks described below.

Mesostasis–olivine–plagioclase rocks. Mesostasis–olivine–plagioclase rocks (M–Ol–P) are more completely crystallized than the devitrified glasses (Fig. 3c). The rocks are dark gray-brown in thin section, the color coming from the mesostasis. Plagioclase (An_{92-95}) forms "H-shaped" crystals that are 2–8 × 30–50 microns in size. In many cases the plagioclase crystals are hollow; hollow centers and ends are filled with mesostasis. The tabular, "H-shaped" plagioclase crystals are typical of quench products with moderate amounts of under-cooling below the

liquidus but well above the solidus (Lofgren, 1973). Olivine (Fo_{75-78}) forms poorly-defined prismatic crystals. Mesostasis forms a "matrix" for the plagioclase and olivine. The mesostasis is cryptocrystalline, consisting of ilmenite or armalcolite, metal, glass, and silicates. Table 4 shows an electron microprobe analysis of the mesostasis from M–Ol–P rock 64535.

Relics are more common than in devitrified glass; they include plagioclase, pink Cr-bearing spinel, and lithic fragments.

M–Ol–P rock grades into mesostasis-rich basalt described below.

Mesostasis-rich basalts. Mesostasis-rich basalts are slightly more completely crystallized than the M–Ol–P rocks. The mesostasis-rich basalts are gray in thin section; dark brown mesostasis is confined to interstitial regions 50 microns across between the silicate crystals (Fig. 3d). The modal abundance of mesostasis (about 15 to 20%) is lower than in the M–Ol–P rocks. The texture is sub-ophitic, except that the mafic phase is olivine and not clinopyroxene.

Plagioclase forms tablet-shaped crystals 3–10 × 40–70 microns in size; they are zoned with a composition ranging from An_{96} to An_{88}. These relations are typical of crystallization with small amounts of under-cooling below the liquidus (Lofgren, 1973). Olivine ranges in composition from Fo_{74} to Fo_{81} and appear to be zoned. It occurs in anhedral crystals (50–80 microns) that are intergrown with plagioclase tablets. Mesostasis is cryptocrystalline, consisting of high-Ca pigeonite (about $Wo_{20}En_{60}Fs_{20}$), ilmenite or armalcolite, metal, and glass. Some of the mesostasis-rich basalts (e.g., 62295) contain tiny (~ 1 micron), rounded octahedra of a pale green Mg–Al spinel in their matrix. Analyses of the mesostasis from two mesostasis-rich diabases (64559 and 64585) are set out in Table 4.

Relics include plagioclase, lithic fragments, pink spinel, and a few olivine crystals.

62295 is a mesostasis-rich basalt that has been studied by many workers (e.g., Agrell *et al.* (1973) and Hodges *et al.* (1973)).

Table 4. Electron microprobe analyses of mesostasis.

	M–Ol–P Rock	Mesostasis-Rich Diabase	
	64535	64559	64585
SiO_2	47.8	52.7	54.5
TiO_2	1.6	0.4	2.8
Al_2O_3	17.1	18.2	14.5
Cr_2O_3	0.1	0.2	0.2
FeO	9.7	6.5	7.0
MgO	14.2	7.4	7.3
CaO	10.5	13.6	13.5
Na_2O	0.6	0.1	0.2
K_2O	0.2	0.4	0.2
Total	101.8	99.5	100.2

Discussion. Although the matrix mineralogy of the mesostasis-rich rocks is essentially constant, other petrographic features define a continuum from devitrified glass to M–Ol–P rock to mesostasis-rich basalt. Plagioclase morphology is spherulitic in the devitrified glasses, skeletal in the M–Ol–P rocks, and tabular in the mesostasis-rich basalts. The series of plagioclase shapes are those expected to crystallize from melts that have experienced progressively less under-cooling (Lofgren, 1973). From devitrified glass to mesostasis-rich basalt there is a trend toward less abundant and better crystallized mesostasis, toward olivine crystals that are more euhedral in shape, and toward a wider range of minerals in the relic assemblage. A higher peak temperature of melting would melt more relics yielding a simple relic assemblage. The above data suggest that the samples at the devitrified glass end of the continuum attained higher peak temperatures followed by more rapid cooling, whereas the samples at the mesostasis-rich basalt end of the continuum attained lower peak temperatures followed by slower cooling.

Basalts

The basalts are sub-ophitic plagioclase-pyroxene plagioclase-pyroxene some of which contain olivine. The texture is dominated by interlocking plagioclase tablets. Pyroxene and olivine crystals are interstitial to the network of plagioclase tablets. Each mafic crystal occupies several adjacent interstitial regions (i.e., the mafic crystals are 2 to 4 times as large as the plagioclase tablets). Metal and Fe–Ti oxides (ilmenite, armalcolite, or ulvöspinel) occupy interstices between the silicates. Pale green Mg–Al spinel occurs as rounded octahedra in plagioclase. Vesicles or vugs that contain few projecting crystals of matrix minerals occur.

In detail, the basalts display a range of textures, mineralogy, and relic population. Four extremes: porphyritic, quenched, metamorphosed, and mafic basalts (Fig. 4) are described below. Pyroxene quadralaterals are shown in Fig. 5.

Porphyritic basalt. Porphyritic basalt is the name given to those rocks with a well defined sub-ophitic texture that contain plagioclase phenocrysts (i.e., the matrix is intergrown with the feldspar megacrysts) and few if any plagioclase relics (Fig. 4a). The only plagioclase relics are similar to those described by Helz and Appleman (1973) from 68415. However, relics of lithic fragments occur. Some of the porphyritic basalts contain textural inhomogenities within their matrix. Patches up to 0.2×1 mm contain the same texture as the remainder of the matrix, only within these patches, the size of the crystals is smaller (or larger) by a factor of 2 to 4. These patches are similar to the cognate inclusions described from 14310 (LSPET, 1971). Rocks 60335, 63545, 63549, 64817, 65055, and 68415–68416 are examples of rocks in this sub-group.

Plagioclase crystals, both phenocrysts and matrix, are zoned with cores near An_{97} and rims as sodic as labradorite. The plagioclase is seriate, ranging in size from tiny euhedral tablets (10×100 microns) to phenocrysts (0.6×10 mm). Compositions of mafic minerals are shown in Figs. 5a, b, and c. Olivine is present in 68415/68416, but not in 63549 and 64817. The pyroxenes in all three start at a

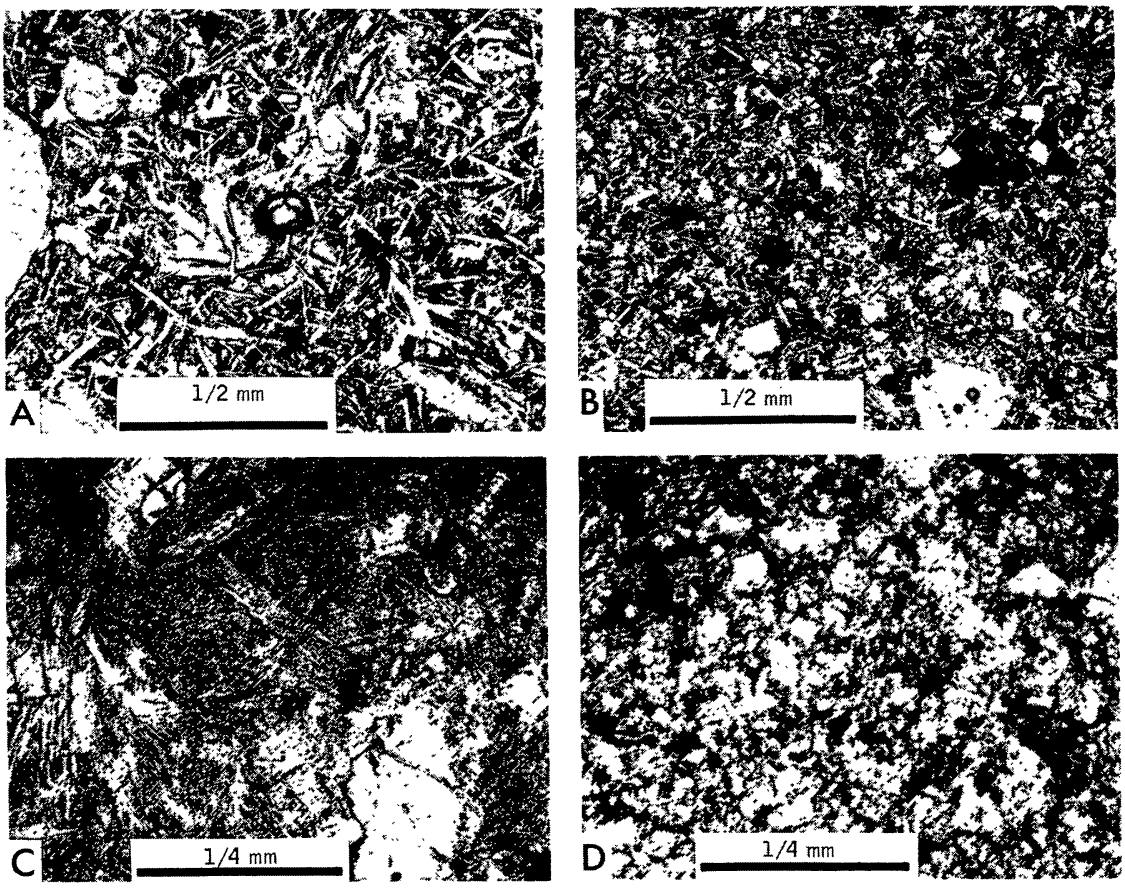

Fig. 4. Photomicrographs of basalts. (a) Porphyritic basalt 63549, note plagioclase phenocrysts; (b) Quench basalt 63535, note the relic megacrysts and the generally "dirtier" appearance than the porphyritic basalt; (c) Metamorphosed basalt 61549, the megacrysts are olivine and plagioclase, the matrix is pyroxene and plagioclase; and (d) Mafic basalt 63598, the grain size of this rock is less than the thickness of the section so the euhedral mineral shapes are somewhat obscured.

Mg-rich, Ca-poor position (orthopyroxene in 68416 and pigeonite in the others), and show a complex fractionation trend that picks up augite and continues to moderate Fe-enrichment. Rusty stains that are common in many Apollo 16 rocks (LSPET, 1973a) are not found in these rocks. Mesostasis makes up less than 2% of the matrix.

It is suggested that the porphyritic basalts are the most likely candidates among the Apollo 16 samples for true igneous rocks, i.e., these rocks may have crystallized from magma that was generated inside the moon rather than in an ejecta blanket. Additional evidence that supports this suggestion is the low Ni content (77 ppm, 60335; 49 ppm, 68415; LSPET, 1973a) of rocks from this group, assuming that Ni contents over 100 ppm are indicative of major meteorite contamination. The quench basalts have Ni contents of greater than 200 ppm (258 ppm, 66095; LSPET, 1973a). Extensive data on siderophile elements (especially Tl and Cs) suggest that most Apollo 16 breccias, including the porphyritic basalts have significant meteoritic contamination (Krahenbuhl *et al.*, 1973).

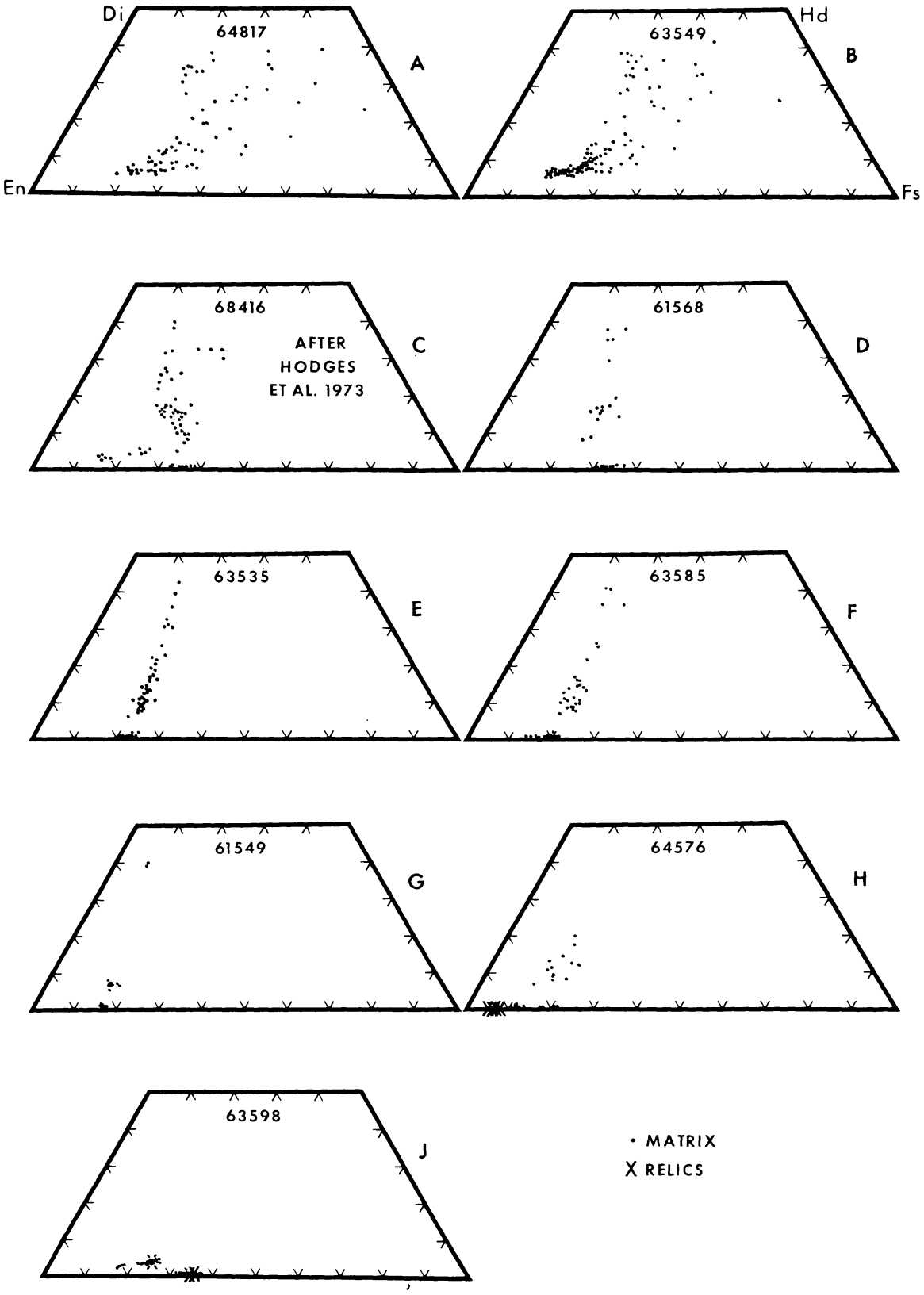

Fig. 5. Pyroxene quadralaterals for matrix pyroxene and olivines from various basalt samples. Olivine composition are plotted along the base.

There are some basalts (61568) that are similar to the porphyritic basalts but they lack phenocrysts and cognate inclusions, and they contain plagioclase relics. The matrix plagioclase (An_{94-98}) is seriate. Mafic mineral compositions are shown in Fig. 5d; they display Fe–Mg distribution coefficients far from unity, but they do not show evidence of extensive fractionation. These rocks are texturally and mineralogically intermediate between the porphyritic and the quench basalts.

Quench basalts. Quench basalt is the name given to those basalts in which the Fe–Mg distribution coefficient among the mafic phases approaches unity. These samples contain relics of lithic fragments, plagioclase, and minor olivine in a sub-ophitic matrix (Fig. 4b). Neither plagioclase phenocrysts nor cognate inclusions have been observed. Rocks 60018, 63506, 63535, 63585, 64435, and 66095 (rusty rock) are examples of rocks in this subgroup.

In the matrix, plagioclase is not extensively zoned; its composition is An_{90-95}. The plagioclase tablets are 10×50 to 20×100 microns in size. Compositions of mafic phases are shown in Figs. 5e and f. Both samples contain olivine, pigeonite, and augite. In each rock the Fe/Mg ratio is about constant within the mafic phases, but the ratio is different in each sample. Similar pyroxene–olivine distributions were observed in some lunar metamorphic rocks from Apollo 14 (Warner, 1972) and Apollo 15 (Phinney *et al.*, 1972 and Cameron *et al.*, 1973). These rocks commonly display a rust stain about the metal particles. Mesostasis makes up between 2 and 5% of the matrix.

In rocks with igneous textures such as these, the observed pyroxene compositions with Fe–Mg distributions near unity and many pyroxenes intermediate between augite and pigeonite are interpreted as the results of quenching. Pyroxenes with compositions consistent with equilibrium crystallization are not observed, suggesting that cooling must have been rapid enough so that crystal-liquid diffusion was limited. The porphyritic basalts contain pyroxenes with compositions that are consistent with equilibrium crystallization, suggesting that they cooled more slowly than the quench basalts.

Metamorphosed basalt. One basalt sample (61549) has been metamorphosed. The compositions of the mafic phases have equilibrated (following Warner's 1972 use of equilibration—all the crystals of a given species have diffused to a single composition) as is shown in Fig. 5g. The texture of this rock reflects the metamorphism. The matrix of the rock consists of prismatic to skeletal olivine crystals (Fo_{82-84}, 50–100 microns) and "H-shaped," skeletal plagioclase tablets (10×100 microns) set in a groundmass of anhedral pyroxene (4–10 microns) and fine-grained plagioclase (Fig. 4c). Immersed in this matrix are abundant plagioclase relics, few pink spinel relics, and one large meta-norite relic. This texture suggests that 61549's protolith was a mesostasis-rich basalt. In fact, if the plagioclase–pyroxene groundmass was a mesostasis the rock would be so classified. Rock 63506 is also classified as metamorphosed basalt.

Mafic basalts. Two rocks are classified as mafic basalts. 64576 and 63598 are different and will be described separately.

The basalt part of 64576 is a vein in a metamorphosed breccia. It consists of olivine (Fo_{90-96}) and plagioclase relics set in a matrix that consists of lath-shaped olivine (2–5 × 60–100 microns; Fo_{79-90}), prismatic pigeonite (10 × 50 microns), and interstitial plagioclase. The compositions of mafic phases are shown in Fig. 5h.

63598 contains abundant, irregular, unlined vesicles in a matrix that consists of subhedral orthopyroxene intergrown with subhedral plagioclase (Fig. 4d). The rock contains plagioclase, olivine, and lithic relics. Plagioclase occurs in 10 × 20 micron tablets and the pyroxene forms 20 × 30 micron prisms. The composition of the mafic phases are shown in Fig. 5j. This sample is very similar to the chief part of 77135 that was described by Warner *et al.* (1973). 63598 is called a micro-norite following the description of 77135.

Discussion. With the exception of the metamorphic basalts, all the basalts contain vesicles and relics of lithic fragments. All but the porphyritic basalts also contain mineral relics of plagioclase, olivine, and pink spinel. These features suggest that these rocks were derived from breccias. Yet, the matrix of the basalts consist of tablet-shaped plagioclase crystals in a sub-ophitic texture with pyroxene and olivine—an igneous texture that crystallized with little or no undercooling. To account for both these constraints, we suggest that the basalts were originally breccias that were heated to almost total melting. Relics were unmelted portions of the original rock. During cooling, the observed matrix texture and mineralogy was formed from the melt. The mineral chemistry suggests that the quench basalts cooled more rapidly than the porphyritic basalts.

Poikilitic rocks

The poikilitic rocks are defined by the poikilitic nature of their matrix texture. The samples consist of oikocrysts, chadacrysts, inter-oikocryst material, and relics (*see* Simonds *et al.*, 1973 and/or Warner *et al.*, 1973 for definitions). Oikocrysts are dominantly pigeonite, orthopyroxene, or olivine, with subordinate augite in some rocks. Chadacrysts are dominantly tablet-shaped, euhedral plagioclase. Augite and olivine also occur as chadacrysts. The regions between oikocrysts consists of tabular plagioclase, olivine, augite, ilmenite or armalcolite, and minor amounts of pale green Mg–Al spinel, metal, sulfide, K-feldspar and apatite. Relics include plagioclase, olivine, pink spinel, and lithic fragments. Vugs and vesicles occur in the poikilitic rocks. The poikilitic rocks are described in detail in our companion paper (Simonds *et al.*, 1973).

The origin of the poikilitic rocks is considered in detail in our Simonds *et al.* (1973) paper where we suggest that the poikilitic rocks formed from the crystallization of an impact-generated melt in an ejecta blanket. We postulate that in order to form a poikilitic texture three criteria must be met: (i) Rock's bulk chemistry must lie near the olivine–plagioclase cotectic surface; (ii) Liquid must undergo a short, rapid temperature drop. The temperature at the end of this drop must be above the intersection of the olivine–pyroxene–plagioclase peritectic; and (iii) Very slow cooling through the above peritectic.

DISCUSSION

A petrogenetic sequence

Six of the lithologies described above (glass, devitrified glass, M–Ol–P rocks, mesostasis-rich basalts, basalts, and poikilitic rocks) define a *petrogenetic sequence* (*see* Table 1). This sequence includes all Apollo 16 rocks that have formed from impact melts. The sequence is characterized by a general increase in crystallinity from the glassy end (which is not crystalline) through intermediate members (which contain skeletal plagioclase crystals and large amounts of mesostasis), to the crystalline end (which contains euhedral plagioclase crystals and small amounts of mesostasis). The lithologies at the glassy end of the petrogenetic sequence display mineral shapes characteristic of large degrees of undercooling, whereas the lithologies at the crystalline end display mineral shapes characteristic of crystallization near the liquidus. This suggests that the lithologies at the glassy end cooled more rapidly than the lithologies at the crystalline end of the sequence.

Several other petrographic features correlate with position in the sequence as are shown in Fig. 6 and outlined below.

Plagioclase shape. In the devitrified glasses plagioclase forms spherulites or dendritic crystals and in the M–Ol–P rocks as "H-shaped" skeletal crystals. Plagioclase occurs as euhedral tablets in the crystalline end of the sequence. Following Lofgren (1973) these data imply plagioclase crystallization at lesser amounts of under-cooling for the rocks at the crystalline end of the sequence.

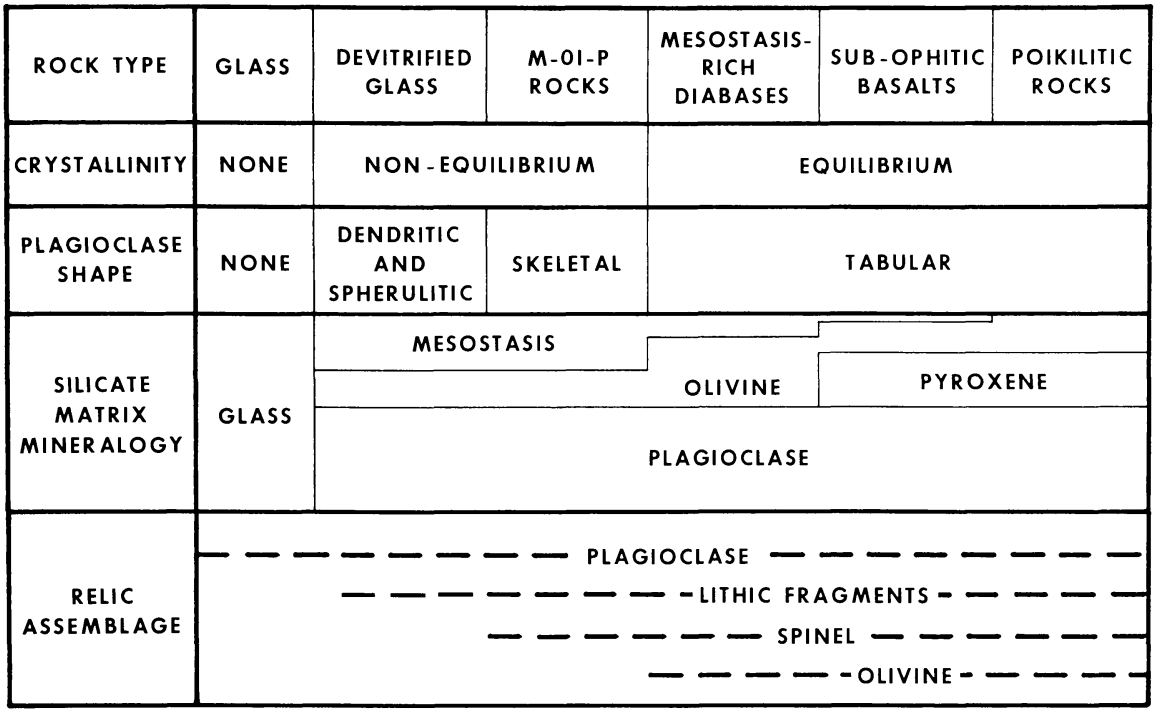

Fig. 6. Chart illustrating systematic petrographic variations in the sequence lithologies. The size of the regions for each phase in silicate matrix mineralogy is schematic.

Silicate matrix mineralogy. As indicated in Fig. 6, the silicate matrix mineralogy is progressively more complex in the crystalline end of the sequence. This is most clear in the change in mesostasis content and the limited range of pyroxene. The occurrence of mesostasis in rocks at the glassy end of the sequence suggests that those rocks crystallized more rapidly than the rocks that lack mesostasis and contain pyroxene.

Relic assemblage. The relic assemblage found for each lithology is shown in Fig. 6. The assemblage becomes more complex at the crystalline end of the sequence. If the relics represent unmelted portions of the protolith, then there is a suggestion that the peak temperature attained was different for the various lithologies in the sequence. We know from Walker *et al.*'s (1973) phase diagram that the sequence of liquidus phases with decreasing temperatures for these rocks are plagioclase, then spinel, then olivine, and finally pyroxene. Since no pyroxene relics were found, the peak temperature for all lithologies must have been greater than the pyroxene melting point. This contrasts to the Apollo 14 meta-breccias that contained abundant pyroxene relics (Warner, 1972). The lack of olivine and spinel relics in the lithologies at the glassy end of the sequence implies that these lithologies attained higher peak temperatures than the lithologies at the crystalline end.

Bulk chemistry

A broad-beam electron microprobe analysis technique was applied to most of the rake samples available. The procedure followed was to open the beam to 210 microns, tune the three crystal spectrometers for Al, Ca, and Fe, and accept data while the sample was driven under the beam at 190 microns per minute. Data were recorded from the crystal spectrometers and from a Si(Li) energy dispersive system. The crystal spectrometer output was used to drive a strip-chart recorder which was visually evaluated in real time to determine when a sufficient amount of sample had been measured to provide a representative analysis. Counting time per sample ranged from $3\frac{1}{2}$ to 20 minutes. Several analyzed lunar rocks were run as tests, and they yield reasonable results. After the broad-beam work was completed, J. M. Rhodes analyzed four of the samples by XRF. These samples also showed that the broad-beam work was acceptable. The Ca/Al ratio agreed within several percent. However, the Fe/Ca ratio derived from the broad-beam work tends to be 5 to 10% lower than the XRF results apparently due to cracks in pyroxenes.

The results of 31 broad-beam analyses of rocks in the sequence are plotted on Fig. 7. For reference some large rocks and average glass compositions are also plotted. All the samples, except the mare basalts, fall on a line from the feldspar composition to a point on the CaO–FeO sideline near the FeO corner. All the Apollo 16 and 17 highland rock analyses (LSPET, 1973a, b) fall on this same trend. These data suggest that to a first approximation the highland rocks may be thought of as a mixture of plagioclase and mafic silicates. The Ca/(Ca+Fe) molar ratio in

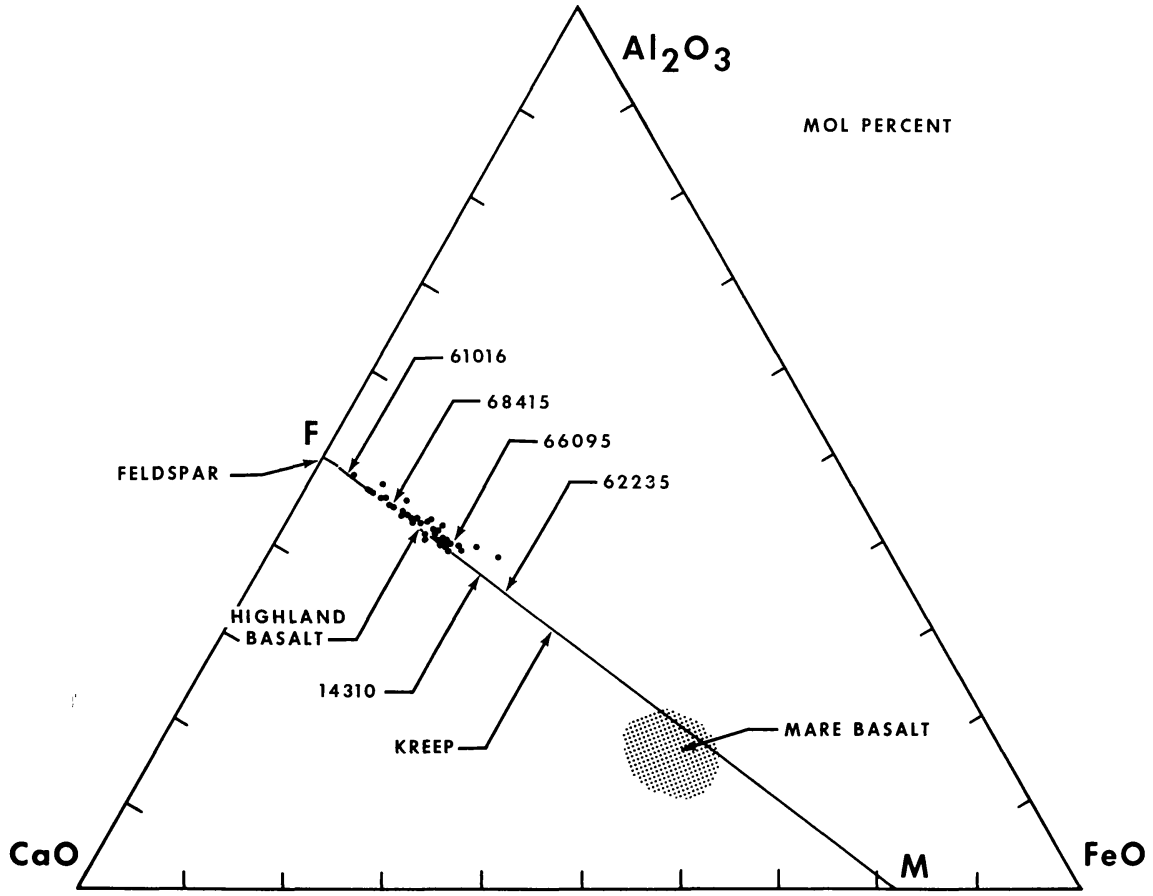

Fig. 7. $CaO–Al_2O_3–FeO$ diagram showing broad-beam analysis of rake samples. Four Apollo 16 large rock analyses (LSPET, 1973a), two average glass compositions (Reid *et al.*, 1972b), a 14310 analysis (LSPET, 1971), and the field of mare basalts are included for reference.

the mafic silicates equals about 0.2- which is a pigeonite, or a mixture of augite and orthopyroxene or olivine. These data show that the textural-mineralogic sequence of lithologies described above also defines a chemically related continuum.

The Apollo 16 and 17 highland rock analyses, plotted on the pseudoternary liquidus diagram of Walker *et al.* (1973) are shown in Fig. 8. A trend is observed from feldspar toward a point on the pyroxene–olivine sideline near pyroxene. This trend is equivalent to the trend illustrated in Fig. 7.

The relevant finding from this bulk chemistry data is that each lithology in the sequence, excepting the poikilitic rocks, covers the full range of compositions. That is, except for the poikilitic rocks, each sequence lithology may be found any place on the composition trend shown in Figs. 7 and 8.

The poikilitic rocks are limited to the mafic end of the spectrum defined by the total sequence. They are confined to compositions near the spinel–plagioclase–olivine peritectic point on Fig. 8. Simonds *et al.* (1973) consider this composition range to be an essential factor in producing poikilitic rocks. From the solid-state detector data, the poikilitic rocks have other unique compositional fea-

tures. Qualitatively, they contain higher TiO_2, P_2O_5, and K_2O than the remaining sequence rocks. The PET analyses (LSPET, 1973a, b) of the large poikilitic rocks confirm this finding. The poikilitic rocks approach the low K Fra Mauro basalt composition of Reid *et al.* (1972a).

Figure 9 is a plot of the broad-beam ratios that are plotted in Fig. 7, projected to the F–M trend line described above. It is clear that these data on our rake samples yield the same results as those derived from Fig. 8.

Glassy breccias as plotted on Figs. 8 and 9 cover the full range of compositions occupied by the sequence lithologies. This relation suggests three possibilities: the glassy breccias are the protolith of the sequence rocks, the glassy breccias were formed from the same protoliths as the sequence lithologies, or the glassy breccias are young rocks that have been locally derived from the sequence lithologies. Some locally derived breccias are undoubtedly present. However, those glassy breccias that have bulk compositions out of the range of soil compositions (*see* Fig. 9 and LSPET, 1973a) cannot be locally derived; they indicate that at least one of the first two suggestions must also be valid. There is no way that we know of to determine if the glassy breccias are the protolith of the sequence lithologies or if they have a common protolith with the sequence lithologies.

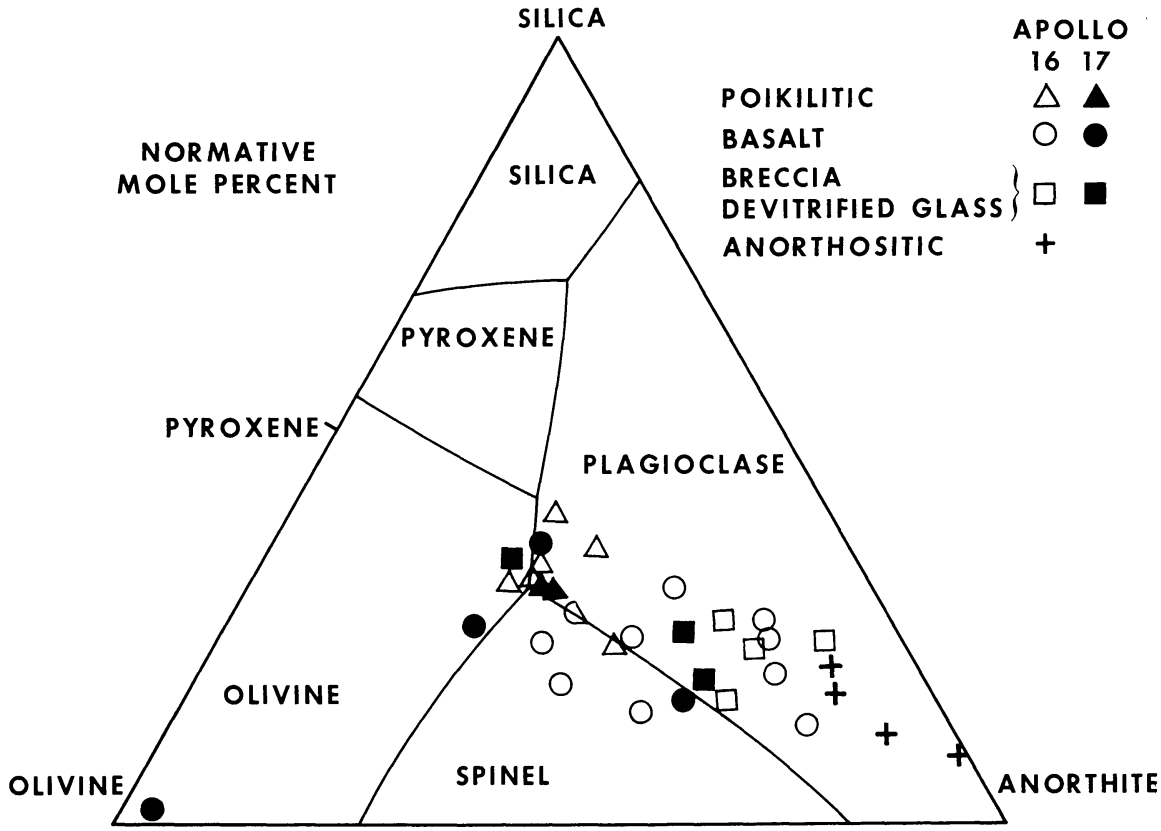

Fig. 8. Apollo 16 and 17 large rock analyses plotted on the olivine–silica–anorthite pseudoternary liquidus diagram of Walker *et al.* (1973). Compositional data from LSPET, 1973a and 1973b.

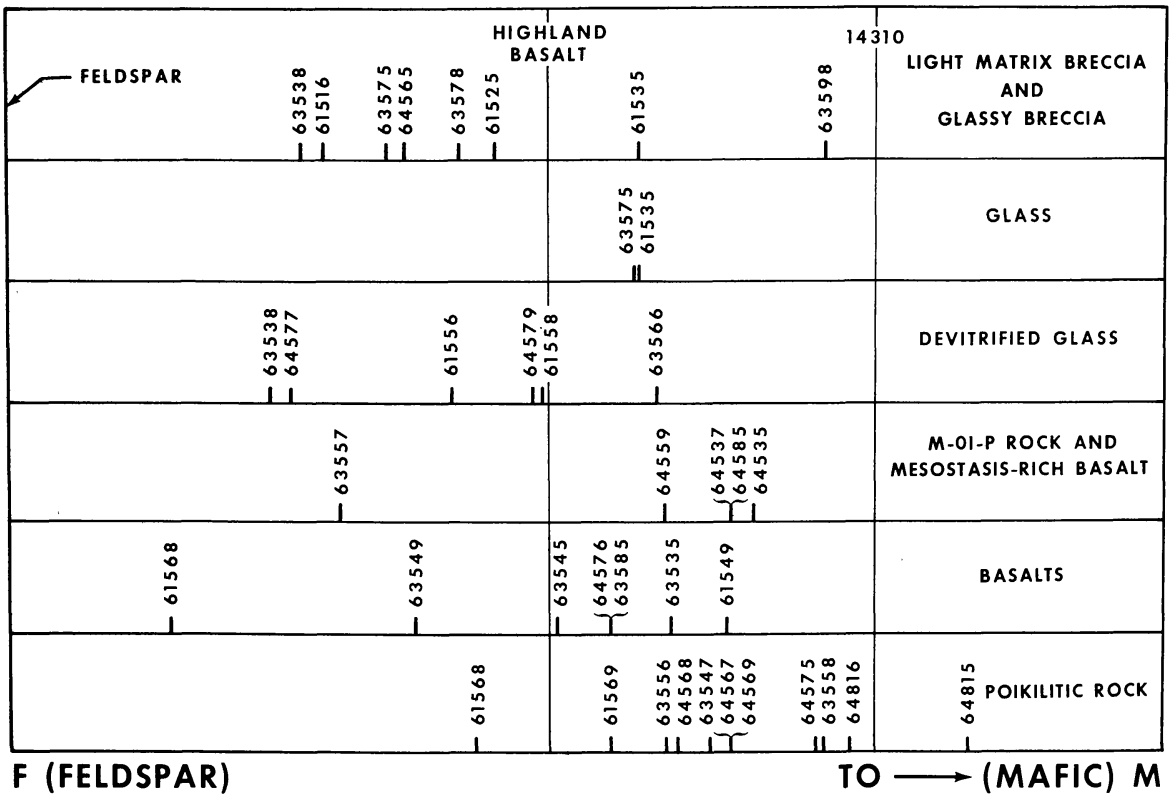

Fig. 9. Broad-beam analyses of rake samples projected normally onto the F-M line shown in Fig. 7. Compositions of highland basalt and 14310 are marked for comparison.

A petrogenetic model

The systematic and continuous nature of the textural and mineralogic changes from glass, through devitrified glass, M–Ol–P rock, mesostasis-rich basalt, and basalt, to the poikilitic rocks suggest a common process of formation. The relevant observations are: (i) all lithologies contain relics, (ii) the matrix mineralogy and texture suggests a melt origin, and (iii) lithologies at the glassy end of the sequence are suggestive of rapid crystallization whereas lithologies from the crystalline end are suggestive of slower crystallization.

Our model consists of two parts (Fig. 10) as follows:

1. Rapid heating of a glassy breccia or unconsolidated mass of regolith in an impact event to about liquidus temperatures. This step produces a melt that contains 5 to 30% relics.

2. Cooling of the hot melt at different rates. The differences among the lithologies in the sequence are due to different cooling rates. Glassy end lithologies cooled rapidly and crystalline end lithologies cooled more slowly. There may be a correlation between peak temperatures and cooling rates; the more rapidly cooled melts attained higher peak temperatures. This may be due to position in the ejecta blanket which may control both variables in a systematic manner.

Some cooling rate limits may be set from experimental data. The glasses must

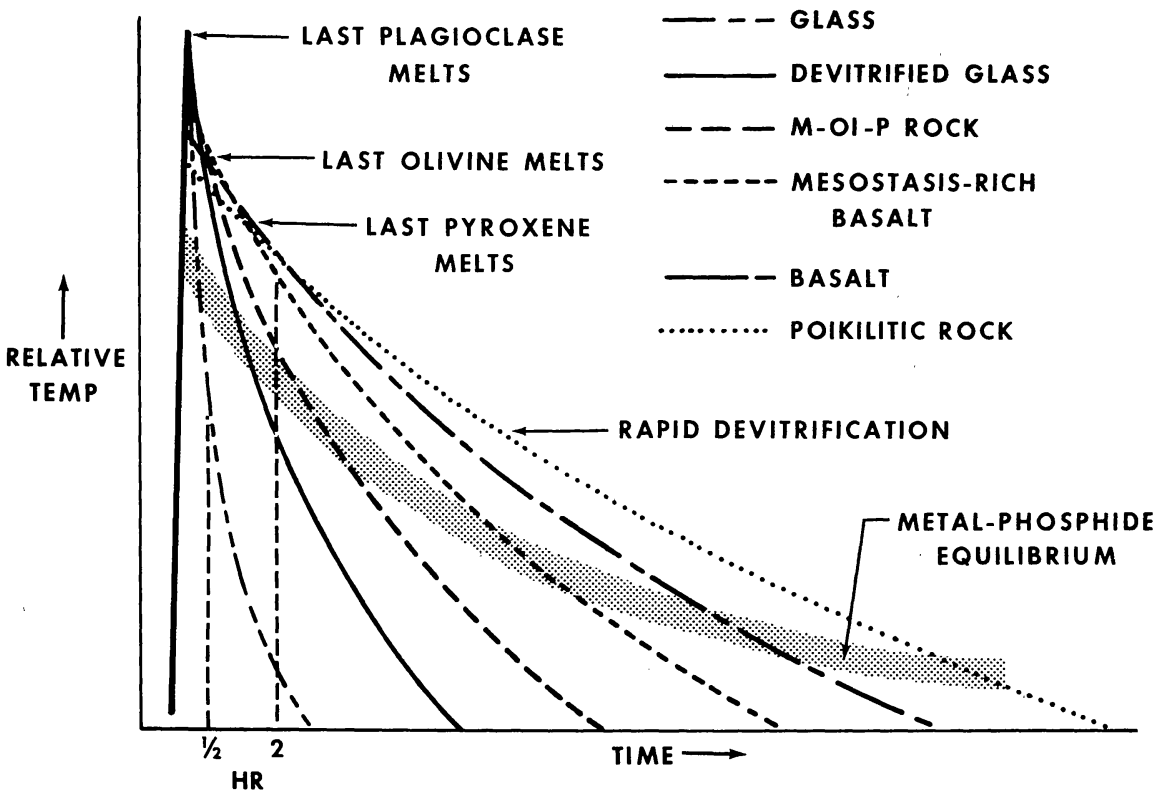

Fig. 10. Diagrammatic sketch illustrating the proposed temperature–time model for impact melted sequence lithologies.

have cooled from a peak temperature near 1300°C to below 700°C in less than ½ hour. Otherwise, the glass would have devitrified (Simonds, 1973). The mesostasis-rich basalts must have cooled to under about 1000°C in less than 2 hours. If longer times are taken the glassy mesostasis will crystallize (Dave Walker, personal comm.). Based on textures in a Fe-metal-schreibersite particle in a poikilitic rock, Gooley *et al.* (1973) have calculated that the rock cooled at a rate equivalent to annealing at 600°C for 4 to 8 weeks. Simonds *et al.* (1973) calculate that the poikilitic rocks cooled from peak temperatures to 1000°C in weeks. Thus independent estimates and measurements of cooling rate agree with the proposed model.

Evidence favoring model

There are several lines of evidence suggesting that all lithologies in the sequence were melted, and that the various lithologies underwent different cooling rates.

Matrix texture. The matrix texture of the sequence lithologies are suggestive of crystallization from a melt or from a glass. Feldspars are accicular, skeletal, or tablet-shaped whereas metamorphic feldspars tend to be equant. Also, the feldspar crystal shapes correlate with position in the sequence as shown in Fig. 6.

The dendritic and spherulitic crystals in the glassy end of the sequence suggest a high degree of under-cooling and thus rapid cooling. The tabular crystals in the crystalline end suggest lesser amounts of under-cooling and thus slower cooling.

Matrix mineralogy. The mineral chemistry, especially in the sub-ophitic basalts and poikilitic rocks, show igneous patterns. Plagioclases are zoned to more sodic compositions. Pyroxenes show two types of trends. The porphyritic basalts and poikilitic rocks display fractionated pyroxene trends and the quench basalts display pyroxene trends suggestive of quenching.

Relic assemblage. Pyroxene relics are not recognized in the sequence lithologies. This lack of pyroxene, in spite of the fact that pyroxene is a major modal/or normative component in the sequence lithologies, suggests that pyroxene was selectively eliminated. Since pyroxene has a lower melting point than the preserved relics (olivine, spinel, and plagioclase), partial melting with peak temperatures above the pyroxene melting point are indicated.

Pore space. Many of the sequence lithologies contain spherical to irregular vesicles with few, if any, projecting crystals. This form of pore space is suggestive of a liquid origin. The unlined vesicles in the Apollo 16 sequence rocks contrasts to the vugs with many projecting crystals that Warner (1972) described from the Apollo 14 metamorphosed breccias.

Metal particles. Metal particles consisting of Fe–Ni metal, troilite, and schreibersite occur in spherical to irregular shapes up to several mm across in the sequence lithologies. Similar metal particles do not occur in glassy breccias or in metamorphic rocks. Gooley *et al.* (1973) have shown that the metal particles are spherical in the glasses and devitrified glasses and irregular in the basalts and poikilitic rocks. These data are compatible with the metal particles being immiscible droplets in a silicate liquid—and the manner in which the silicates crystallized controlled the final shape of the metal particles. That is, in the rapidly cooled lithologies, the spherical shape of the metal droplet was quenched in, whereas in the more slowly cooled lithologies the silicate crystals deformed the metal droplets.

Metal-phosphide equilibrium. Gooley *et al.* (1973) have also studied the Fe–Ni metal-schreibersite equilibrium as a function of host rock lithology. They show that the final equilibration was above 1000°C in the devitrified glasses, about 650°C in the mesostasis-rich basalts, about 550°C in the basalts, and below 500°C in the poikilitic rocks. These progressively lower equilibration temperatures are interpreted as indicating different cooling rates: the lithologies with higher equilibrium temperatures cooled rapidly whereas the lithologies with low equilibrium temperatures cooled more slowly.

Poikilitic rocks. The poikilitic rocks are the most questionable lithology in the sequence as to a melt origin. However, Simonds *et al.* (1973) present compelling arguments that the poikilitic rocks are, in fact, of igneous origin.

Melted matrix breccias. The melted matrix breccias constitute an important group of rocks as they form an intermediate member between pristine glassy or metamorphic breccias and the more fully melted lithologies in the sequence. The existence of melted matrix breccias are a strong indication that glassy or metamorphic breccias were the protolith of the various sequence lithologies.

Cataclastic anorthosite. The cataclastic anorthosites contain angular regions consisting of lath-shaped feldspar and pyroxene. These "basaltic" patches are interpreted as evidence of partial melting (LSPET, 1973a). These patches, like the melted matrix breccias, show that melting was a widespread phenomenon in the ejecta blankets that make up the Apollo 16 site.

Epilogue

Before being able to make full use of the highland rocks in interpreting the moon's evolution, the detailed petrogenesis of the samples must be unraveled. Since most returned highland rocks are breccias that are the product of impact processes, those processes must be understood. In this paper we have studied the Apollo 16 rocks and have demonstrated that they were formed from impact generated partial melts. Our previous papers (Warner, 1972; Phinney *et al.*, 1972) studied the Apollo 14 rocks that were metamorphosed but not melted, and the Apollo 15 Front rocks that were neither melted nor metamorphosed. Cursory examination of the Apollo 17 Massif rocks (Warner *et al.*, 1973) suggests that they are similar to the Apollo 16 rocks in general petrogenesis. An integration of the data from Apollos 14 and 17 should yield significant advances in our understanding of the petrogenetic processes that take place as a result of major impacts. This will lead to a better comprehension of the highlands, and thus the moon. The stage is set and we have received our cue.

Acknowledgments—A portion of the research reported in this paper was done while one of the authors (C.H.S.) was a Visiting Post-doctoral Fellow at the Lunar Science Institute which is operated by the Universities Space Research Association under Contract No. NSR 09-051-001 with the National Aeronautics and Space Administration. This paper constitutes Lunar Science Contribution No. 147.

References

Agrell S. O., Agrell J. E., Arnold A. R., and Long J. V. P. (1973) Some observations on rock 62295. In *Lunar Science—IV*, pp. 15-17. The Lunar Science Institute, Houston.

Cameron K. L., Delano J. W., Bence A. E., and Papike J. J. (1973) Petrology of the 2–4 mm soil fraction from the Hadley-Apennine region of the moon. *Earth Planet. Sci. Lett.* **19**, 9–21.

Delano J. W., Bence A. E., Papike J. J., and Cameron K. (1973) Petrology of the 2–4 mm soil fraction from Apollo 16. In *Lunar Science—IV*, pp. 172–174. The Lunar Science Institute, Houston.

Domenico P. A. (1972) Concepts and models in groundwater hydrology. 405 pp. McGraw-Hill, New York.

Gooley R., Brett R., and Warner J. L. (1973) Crystallization history of metal particles in Apollo 16 rake samples. *Proc. Fourth Lunar Sci. Conf., Geochim. Cosmochim. Acta.* This volume.

Helz R. T. and Appleman D. E. (1973) Mineralogy, petrology and crystallization history of Apollo 16 sample 68415 (abstract). In *Lunar Science—IV*, pp. 352–354. The Lunar Science Institute, Houston.

Hodges F. N., Kushiro I., and Seitz M. G. (1973) Petrology of lunar highland rocks of Apollo 16 (abstract). In *Lunar Science—IV*, pp. 371–373. The Lunar Science Institute, Houston.

James O. B. (1972) Lunar anorthosite 15415: Texture, mineralogy, and metamorphic history. *Science* **175**, 432–436.

Krahenbuhl U., Ganapathy R., Morgan J. W., and Anders E. (1973) Volatile elements in Apollo 16 samples: Possible evidence for outgassing of the moon. *Science* **180**, 858–861.

Lofgren G. (1973) An experimental study of plagioclase crystal morphology. *Am. J. Sci.* In press.

LSPET (Lunar Sample Preliminary Examination Team) (1971) Preliminary examination of lunar samples from Apollo 14. *Science* **173**, 681–693.

LSPET (Lunar Sample Preliminary Examination Team) (1973a) Preliminary examination of lunar samples from Apollo 16. *Science* **179**, 23–34.

LSPET (Lunar Sample Preliminary Examination Team) (1973b) Preliminary examination of lunar samples from Apollo 17. *Science.* In press.

McKay D. S. and Morrison D. A. (1971) Lunar breccias. *J. Geophys. Res.* **76**, 5658–5669.

Phinney W. C., Warner J. L., Simonds C. H., and Lofgren G. E. (1972) Classification and distribution of rock types at Spur Crater. *The Apollo 15 Lunar Samples*, pp. 149–153. The Lunar Science Institute, Houston.

Reid A. M., Warner J., Ridley W. I., and Brown R. W. (1972a) Major element composition of glasses in three Apollo 15 soils. *Meteoritics* **7**, 395–415.

Reid A. M., Warner J. L., Ridley W. I., Johnson D. A., Harmon R. S., Jakes P., and Brown R. W. (1972b) The major element composition of lunar rocks as inferred from glass compositions in the lunar soil. *Proc. Third Lunar Sci. Conf., Geochim. Cosmochim. Acta*, Suppl. 3, Vol. 1, pp. 363–378. MIT Press.

Simonds C. H. (1973) Sintering and hot pressing of Fra Mauro composition glass and the lithification of lunar breccias. *Am. J. Sci.* **273**, 428–439.

Simonds C. H., Warner J. L., and Phinney W. C. (1973) Petrology of Apollo 16 poikilitic rocks. *Proc. Fourth Lunar Sci. Conf., Geochim. Cosmochim. Acta.* This volume.

Walker D., Longhi J., and Hays J. F. (1973) Petrology of Apollo 16 metaigneous rocks. In *Lunar Science—IV*, pp. 752–754. The Lunar Science Institute, Houston.

Warner J. L. (1972) Metamorphism of Apollo 14 breccias. *Proc. Third Lunar Sci. Conf., Geochim. Cosmochim. Acta*, Suppl. 3, Vol. 1, pp. 623–643. MIT Press.

Warner J. L., Simonds C. H., Phinney W. C., and Gooley R. (1973) Petrology and genesis of two "igneous" rocks from Apollo 17 (76055 and 77135). *EOS* **54**, 620–621.

Wilshire H. G., Stuart-Alexander D. E., and Jackson E. D. (1973) Petrology and classification of the Apollo 16 samples. In *Lunar Science—IV*, pp. 784–786. The Lunar Science Institute, Houston.

Wood J. A., Dickey J. S., Marvin U. B., and Powell B. N. (1970) Lunar anorthosites and a geophysical model of the moon. *Proc. Apollo 11 Lunar Sci. Conf., Geochim. Cosmochim. Acta*, Suppl. 1, Vol. 1, pp. 965–988. Pergamon.